Geomorphology and development of a high-latitude channel system: the INBIS channel case (NW Barents Sea, Arctic)

L. Rui, M. Rebesco, J. L. Casamor, J. S. Laberg, T. A. Rydningen, A. Caburlotto, M. Forwick, R. Urgeles, D. Accettella, R. G. Lucchi, et al.

arktos
The Journal of Arctic Geosciences

ISSN 2364-9453

Arktos
DOI 10.1007/s41063-019-00065-9

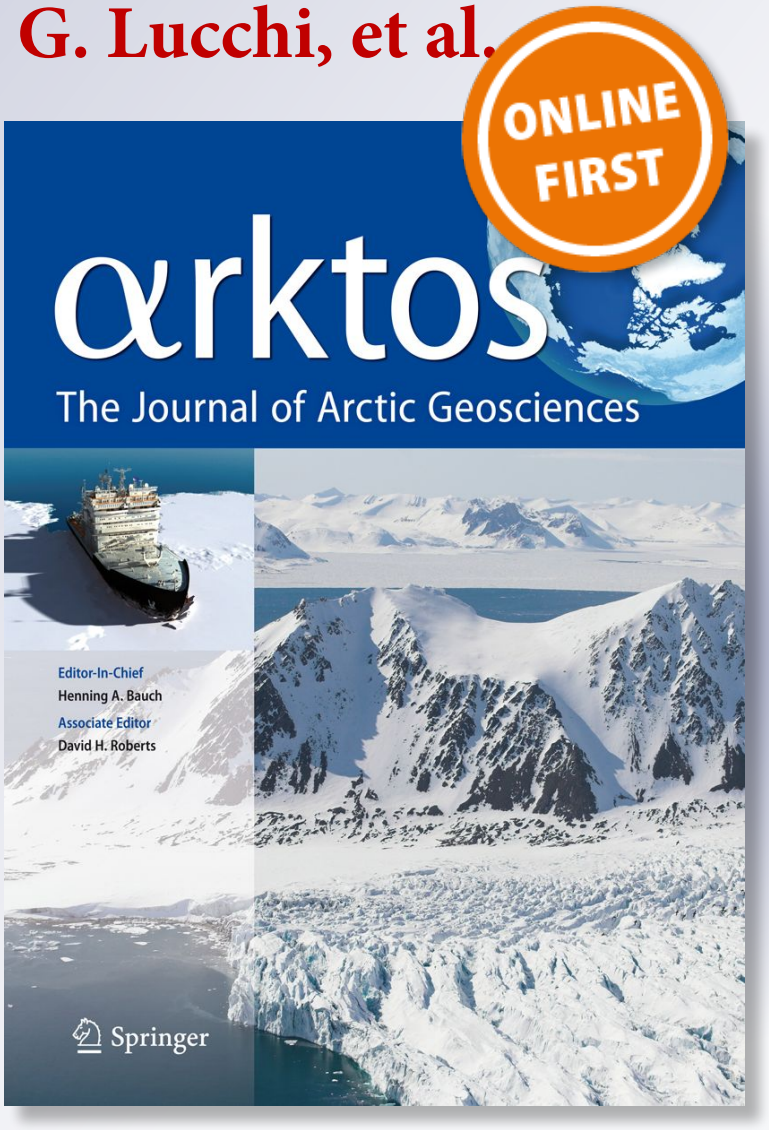

Springer

arktos
https://doi.org/10.1007/s41063-019-00065-9

ORIGINAL ARTICLE

Geomorphology and development of a high-latitude channel system: the INBIS channel case (NW Barents Sea, Arctic)

L. Rui[1,7] · M. Rebesco[1] · J. L. Casamor[2] · J. S. Laberg[4] · T. A. Rydningen[4] · A. Caburlotto[1] · M. Forwick[4] · R. Urgeles[3] · D. Accettella[1] · R. G. Lucchi[1] · I. Delbono[5] · M. Barsanti[5] · M. Demarte[6] · R. Ivaldi[6]

Received: 1 September 2018 / Accepted: 13 February 2019

Abstract

The INBIS (Interfan Bear Island and Storfjorden) channel system is a rare example of a deep-sea channel on a glaciated margin. The system is located between two trough mouth fans (TMFs) on the continental slope of the NW Barents Sea: the Bear Island and the Storfjorden–Kveithola TMFs. New bathymetric data in the upper part of this channel system show a series of gullies that incise the shelf break and minor tributary channels on the upper part of the continental slope. These gullies and channels appear far more developed than those on the rest of the NW Barents Sea margin, increasing in size downslope and eventually merging into the INBIS channel. Morphological evidence suggests that the Northern part of the INBIS channel system preserved its original morphology over the last glacial maximum (LGM), whereas the Southern part experienced the emplacement of mass transport glacigenic debris that obliterated the original morphology. Radiometric analyses were applied on two sediment cores to estimate the recent (~ 110 years) sedimentation rates. Furthermore, analysis of grain size characteristics and sediment composition of two cores shows evidence of turbidity currents. We associate these turbidity currents with density-driven plumes, linked to the release of meltwater at the ice-sheet grounding line, cascading down the slope. This type of density current would contribute to the erosion and/ or preservation of the gullies' morphologies during the present interglacial. We infer that Bear Island and the shallow morphology around it prevented the flow of ice streams to the shelf edge in this area, working as a pin (fastener) for the surrounding ice and allowing for the development of the INBIS channel system on the inter-ice stream part of the slope. The INBIS channel system was protected from the burial by high rates of ice-stream derived sedimentation and only partially affected by the local emplacement of glacial debris, which instead dominated on the neighbouring TMF systems.

Keywords INBIS · Channel system · Barents Sea · Trough mouth fans · Glaciated margin · ^{210}Pb dating method

Introduction

Reconstruction of paleo-ice stream behaviour on a high-latitude glaciated continental margin is possible through the analysis of the associated characteristic features in the sedimentological and geomorphological record [82]. The most prominent features related to the activity of ice streams are the trough mouth fans (TMFs). These prograding fan-shaped sediment wedges are formed by glacigenic debris flows discharged by paleo-ice streams [83]. Gullies are small V-shaped erosional features that dissect the shelf edge and upper continental slope [29, 55]. On high-latitude margins, potential gully-forming erosive mechanisms are: sediment-laden subglacial meltwater, discharged from the ice sheet, mainly during deglaciations [22, 48, 50, 55, 92]; dense bottom waters produced through sea-ice formation and

✉ L. Rui
leorui89@gmail.com

1 OGS Istituto Nazionale di Oceanografia e di Geofisica Sperimentale, Sgonico, TS, Italy

2 GRC Geociències Marines, Universitat de Barcelona, Barcelona, Spain

3 Institut de Ciències del Mar, Consejo Superior de Investigaciones Científicas, Barcelona, Spain

4 Department of Geosciences, UiT The Arctic University of Norway in Tromsø, Tromsö, Norway

5 Marine Environment Research Centre, ENEA, La Spezia, Italy

6 Italian Navy Hydrographic Institute, Genoa, Italy

7 University of Trieste, Trieste, Italy

Published online: 25 February 2019

brine rejection [85]; turbidity currents [26]; iceberg scouring [23] and glacigenic sediment flows [20, 21]. If the processes responsible for the formation of gullies are persistent over time and/or increase in intensity, they can lead to the formation of canyon–channel systems. These are larger net erosional to net depositional features that dissect the shelf edge and extend across the seafloor from the continental shelf into the deep ocean [1, 2, 14, 31, 57]. The downslope part of these systems can eventually evolve into U-shaped, lower-relief channels across the lower continental slope and beyond [56, 80].

It is important to study underwater channel systems as they are the preferred route for the offshore transport of sediment, nutrients and dense water masses. These systems are effectively carved by dense water and sediment gravity flows, delivering material from the shelf edge to the deep sea, particularly during sea-level low-stand periods [31]. Therefore, the presence and the morphology of a channel system affect the growth and the evolution of the continental margin and vice versa. On presently or formerly glaciated continental margins, the development of channel systems, aside from TMFs, is attributed to several mechanisms related to the cycles of advances and retreats of past ice sheets. Therefore, the study of high-latitude channel systems could lead to a better understanding of the dynamics of ice build-up and retreat and associated glacigenic sediment transport during these periods. Moreover, the study of high-resolution data is essential to increase our understanding on the spatial and temporal variability of glacimarine processes operating on high-latitude margins (e.g. [59]). In fact, a marked lateral sedimentary variability of sedimentary processes due to local physiography and hydrodynamics has been highlighted for this study area by Zecchin et al. [93].

The aim of this paper is to increase our understanding on the development of this part of the continental margin during the late Quaternary. To achieve this aim we will: (1) study the morphology and the bathymetry of the INBIS channel system; (2) assess the role of down-slope and along-slope processes in the channel system evolution; (3) identify the genetic mechanisms of the INBIS channel system and its interactions with the nearby TMF systems.

Geological background and evolution of the Svalbard–Barents–Kara ice-sheet (SBKIS)

Several studies have been conducted to reconstruct the timing and dynamics of the deglaciation of the NW Barents Sea and western Svalbard continental margins after the LGM [24, 34, 37, 68–70, 75, 91, 78, 91, 68, 37, 69, 70, 75]. Although the dynamics and exact timing of the deglaciation are still a matter of debate, there is agreement that the glacial retreat started in the deeper troughs due to the influence of ocean warming and sea-level rise [38, 46, 76, 90]. The last glacial maximum (LGM) in the area of the NW Barents sea occurred around 23–19 ka, with the maximum ice extent reached at around 21.5 ka [62]. At that time the Barents Sea Ice Sheet extended to the shelf edge of the western Barents Sea margin with areas of fast-flowing ice streams in the troughs and slower-flowing ice on the shallower banks [84]. The onset of the deglaciation is inferred to have begun around 20–19 ka in the outermost part of west Spitsbergenbanken [24, 68] and in the Kveithola Trough [50, 65, 69, 71]. The deglaciation occurred as an alternation of rapid retreats, still stand periods and/or re-advances [65, 68, 69, 71, 76, 11, 12, 76]. In the Bear Island Trough, the ice stream started its retreat around 19.5 ka [63]. However, it is inferred to have re-advanced hundreds of kilometres toward the shelf break at least three times before 17.8 ka [63] and at around 17.1 ka [75] before starting its final, stepwise retreat [5, 6, 90]. In the final stages, the combination of abrupt sea-level rise and ocean warming triggered a retreat of 145 km in 700 years, followed by the final decay of the ice stream by 13 ka [66]. The Bear Island (Bjørnøya), located between the Storfjorden and Bear Island Troughs, was ice-free at 11.2 cal. ka BP [91].

There are few systematic studies of channel systems on glaciated continental margins. A channel system on the East Greenland continental margin, in front of the Kaiser Franz Joseph Fjord, is inferred to be the oldest channel in the Norwegian–Greenland Sea [21, 30, 53, 64, 89; 58, 89, 30, 64]. The start of the formation of this channel is dated to around 2.5 Ma [89]. It originates at a water depth of about 1500 m on the continental slope, crosses glacigenic debris flow deposits located on the lower part of the slope and extends north-east for 500 km, terminating in the Greenland Basin at a water depth of 3700 m [89]. The formation of this channel system is mainly attributed to sediment-laden meltwater produced by the eastern Greenland ice sheet. Along the Norwegian and Svalbard continental margin, channel systems are less developed compared to the East Greenland continental margin [89]. So far, three large deep-sea channel systems have been described: the Lofoten Basin Channel System [19, 72, 85], formed by the 30-km-long Andøya Canyon and its continuation, a 300-km-long channel located in the SE Lofoten Basin, reaching a water depth of 3000 m [3, 45]; the Kongsfjorden channel system [27], a ~ 120-km-long channel system located on the continental slope off northwest Svalbard, between water depths of ~ 250–4000 m; and the INBIS channel system [85, 86] located on the continental slope west of Bear Island (NW Barents Sea) (Fig. 1).

The INBIS Channel is a 60-km long and 5–15-km wide, nearly flat-bottomed east–west oriented channel, located between water depths of ~ 2350–2520 m (Fig. 2). Vorren et al. [85] attribute the formation of the INBIS Channel to

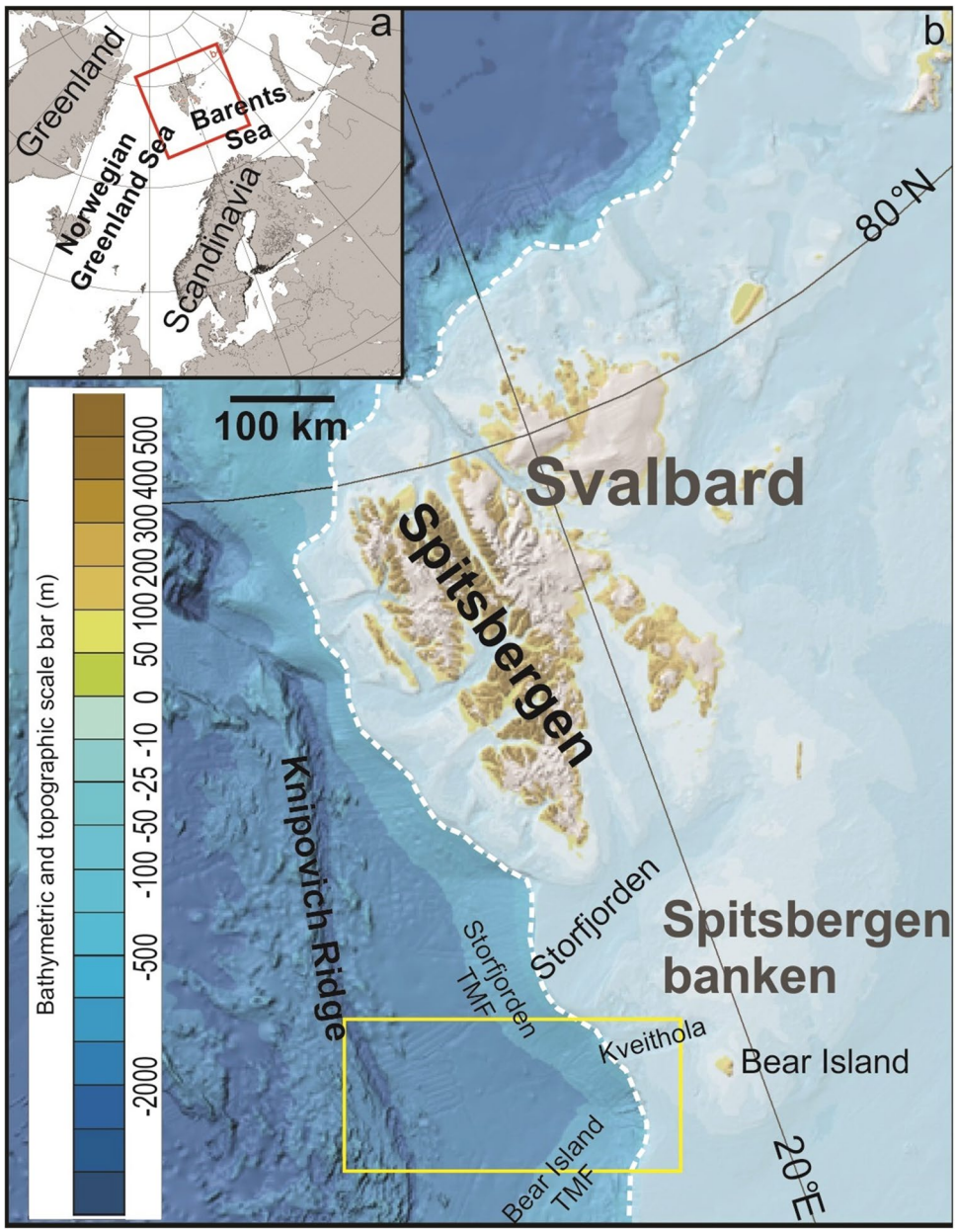

Fig. 1 **a** Map of the Arctic Ocean. The red square indicates the location of **b. b** Map of the NW Barents Sea based on the International Bathymetric Chart of the Arctic Ocean (IBCAO) [36]. The area of study is indicated by a yellow rectangle (Fig. 2). The dashed white line represents the extension of the Svalbard–Barents–Kara ice sheet (SBKIS) during the last glacial maximum (LGM) [33]

density-driven currents descending the southern flank of the Storfjorden TMF, the northern flank of the Bear Island TMF and the inter-TMF area between these two TMFs. At that time, no bathymetry data were available to show the large influence of the Kveithola TMF on the location of the INBIS Channel System. Core analysis (GK 23257 in Vorren et al. [85]) suggests that these density-driven currents were active mainly during glaciations. The origin of these density-driven currents is attributed to dense water formed by cooling under sea-ice formation with brine rejection, or to turbidity currents generated from small landslides on the upper slope. The INBIS Channel is partially infilled by glacigenic debris flows, which reached their main activity during glacial maxima [84, 85].

Data and methods

Data acquisition was carried out during four main oceanographic cruises: the EGLACOM (Evolution of a GLacial Arctic COntinental Margin, July–August 2008) and the DEGLABAR (DEGLAciation History of the North-Western BARents Sea from Sediments Generated by Paleo-Ice Streams Deglaciation history of the NW BARents Sea, September 2015) cruises, both on board the Italian R/V OGS Explora; the CORIBAR (CORIng in the NW BARents Sea, July–August 2013) cruise on board the German R/V Maria S. Merian; and the HN17 (High North 17, July 2017) cruise on board the NATO-MMI R/V Alliance. Swath bathymetry data were acquired during the main four cruises (see

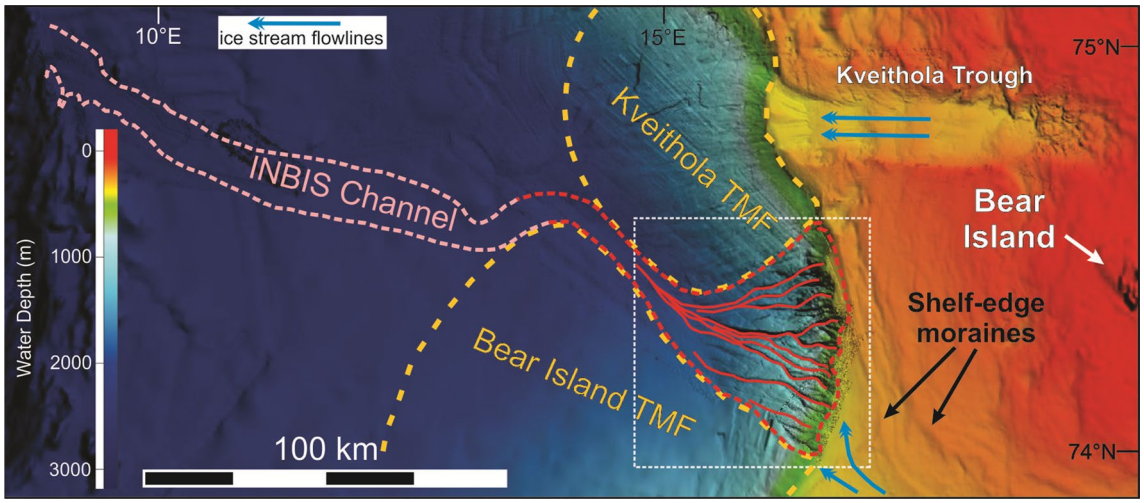

Fig. 2 Bathymetric map of the INBIS channel system area. This map has been produced with all available multibeam datasets, superimposed onto IBCAO [36]. The white dotted square marks the inter-TMF area analysed in this paper (see Fig. 3a, b). Red lines highlight the major channels, while the dashed red lines infer the maximum extension of the upper part area of the system. The dashed pink line represents the INBIS Channel described by Vorren et al. [85]. The Kveithola and Bear Island TMFs are depicted by a yellow dashed line. Moraines, between 2 and 5 km from the shelf edge, represent the outer shelf limit of grounded slow-moving ice during the LGM (cf. Fig. 7c)

Table 1), and three box cores were collected in the INBIS Channel System area during HN17, providing indications of modern sedimentary environments in the study area. In addition, a minor part of Swath bathymetry data was acquired during the SVAIS [13] and GlaciBar [4] cruises.

Swath bathymetry

The swath bathymetry data collected during the EGLACOM and DEGLABAR cruises were acquired using Multibeam Echosounders (MBES) Reson MB8111–MB8150 and Reson MB8111–MB7150, respectively. During the CORIBAR cruise, the swath bathymetry data were collected with Kongsberg EM1002 and EM 122 MBES, whereas the MBES Kongsberg EM 302 was used during the HN17 cruise. All systems used were hull-mounted and had a swath of 150°.

The acquired data were processed using PDS2000 and CARIS. The processed data were merged into one dataset with a cell size of 30 m. During the last days of the DEGLABAR cruise, rough weather conditions affected the acquisition of bathymetric data, resulting in considerably lower data quality in the southernmost part of the INBIS Channel System.

Ground truthing

Ground truthing was performed at three sites using a box corer assembled with a box sized 30 × 20 × 50 cm, working with a 125 kg weighted head. The sediment box was subsampled with plastic liners for shore-based analyses. Each sediment core was logged visually (sediment colour code according to the Munsell Colour Chart) and by X-radiography. Physical properties were measured at 1-cm resolution with a multi-sensor core logger (P-wave velocity, wet bulk density, and loop sensor magnetic susceptibility). Qualitative element-geochemical measurements were performed with an Avaatech X-ray fluorescence (XRF) core scanner for light (10 kV) and heavy (30 kV) elements at 1-cm resolution. The results of the XRF core scanning are presented as calcium vs titanium ratio (Ca/Ti), giving indication of biological carbonate versus terrigenous sediment input (e.g. [17]). Following Wang et al. [88] and Caricchi et al. [15], the zirconium vs rubidium ratio (Zr/Rb) was used as a qualitative indicator of the grain size characteristics as Zr is usually contained in sand-sized sediment, whereas Rb is an element that is typically contained in clay minerals (c.f. [15, 88]).

Radiometric analyses and dating model

Sediment cores HN17-07BC2 and HN17-08BC3 (Fig. 4) were sliced at 1 cm resolution for Gamma ray spectrometry analyses carried out at ENEA Marine Environment Research Centre La Spezia (Italy), according to the methods described by Delbono et al. [18].

$^{210}Pb_{xs}$ and ^{137}Cs activities are measured in Bq kg^{-1} sediment dry weight. ^{210}Pb dating method has been widely used for establishing geochronology in marine sediments, so that Sediment Accumulation Rate (SAR, cm $year^{-1}$) can be estimated, on time scales of ~ 110 years, compatible with ^{210}Pb physical half-life [8, 41, 74, 79]. Among the typically

used dating models based on $^{210}Pb_{xs}$ profiles, in this paper, we apply the CRS model that assumes a constant rate of supply of $^{210}Pb_{xs}$ [7]. The down-core ^{137}Cs activity profiles are often used as an independent validation of ^{210}Pb dating models [81], since they provide a similar clock with some well-defined temporal features such as the 1963 fallout peak (associated to nuclear bomb testing) and the 1986 Chernobyl peak [16, 73].

Results

The studied area of the INBIS Channel System is divided into three morphological areas: (1) the upper reaches of the channel, (2) the northern and (3) southern sectors of the middle slope (Fig. 3).

The upper reaches of the INBIS channel system

The upper reaches of the INBIS channel system have an amphitheatre shape extending from the Kveithola to the Bear Island TMFs (Fig. 2) for ca. 60 km. This gully-dominated part extends from the shelf edge, at a depth of ca. 420 m to a water depth ranging from 700 m in the north of the amphitheatre to 1100 m in the south. Further downslope the INBIS channel system develops into a channel-dominated part. Along the upper reaches, it is possible to identify 40 gullies with an average axial dip of 4°–5°. The gullies are characterized by an overall V-shape (Fig. 5), with widths varying from 150 to 600 m, and incision depths varying from 10 to 60 m. The gullies originate at the shelf edge, with a lateral spacing of 450–950 m in the northern area, increasing to approximately 2 km in the southern area (Fig. 3). The

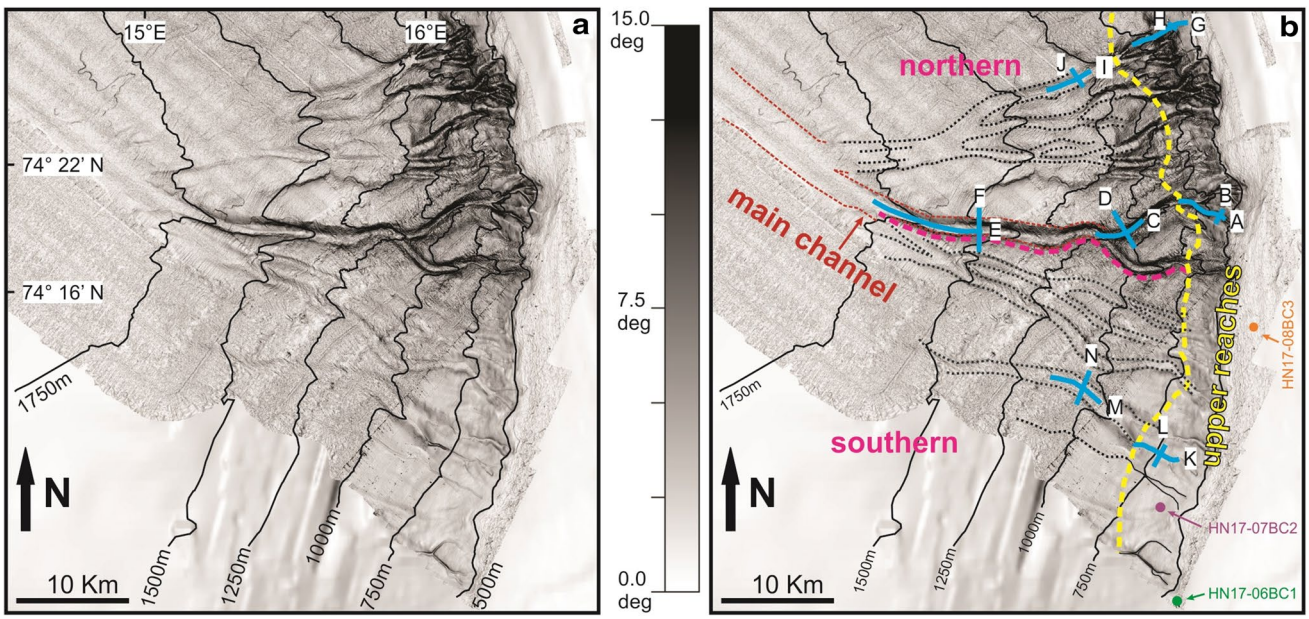

Fig. 3 Slope gradient maps, uninterpreted (**a**) and interpreted (**b**) of the parts of INBIS Channel System analysed in this paper (white dotted square in Fig. 2). The INBIS Channel System is divided into upper reaches (limited by the dashed yellow line), northern and southern parts (separated by the dashed pink line). Bathymetric sections in dip directions (A, C, E, G, I, K and M) and in strike directions (B, D, F, H, J, L and N) are depicted in light blue. Six less visible channels are highlighted with dotted black lines. The main channel is highlighted by a dashed red line. The location of cores HN17-06BC1, HN17-07BC2 and HN17-08BC3, collected during High North 17 cruise is depicted in green, purple and orange, respectively

Table 1 List of the multibeam systems used by name, acquisition year, cruise, research vessel, operating frequency and beam number

Name	Acquisition year	Cruise(s)	Research vessels	Operating frequency	Beam number
MB8111	2008/2015	EGLACOM / DEGLABAR	OGS Explora	100 kHz	101
MB8150	2008	EGLACOM	OGS Explora	12 kHz	234
MB7150	2015	DEGLABAR	OGS Explora	12 kHz	880
EM1002	2013	CORIBAR	Maria S. Merian	95 kHz	111
EM122	2013	CORIBAR	Maria S. Merian	12 kHz	432
EM302	2017	High North 17	NRV Alliance	30 kHz	864

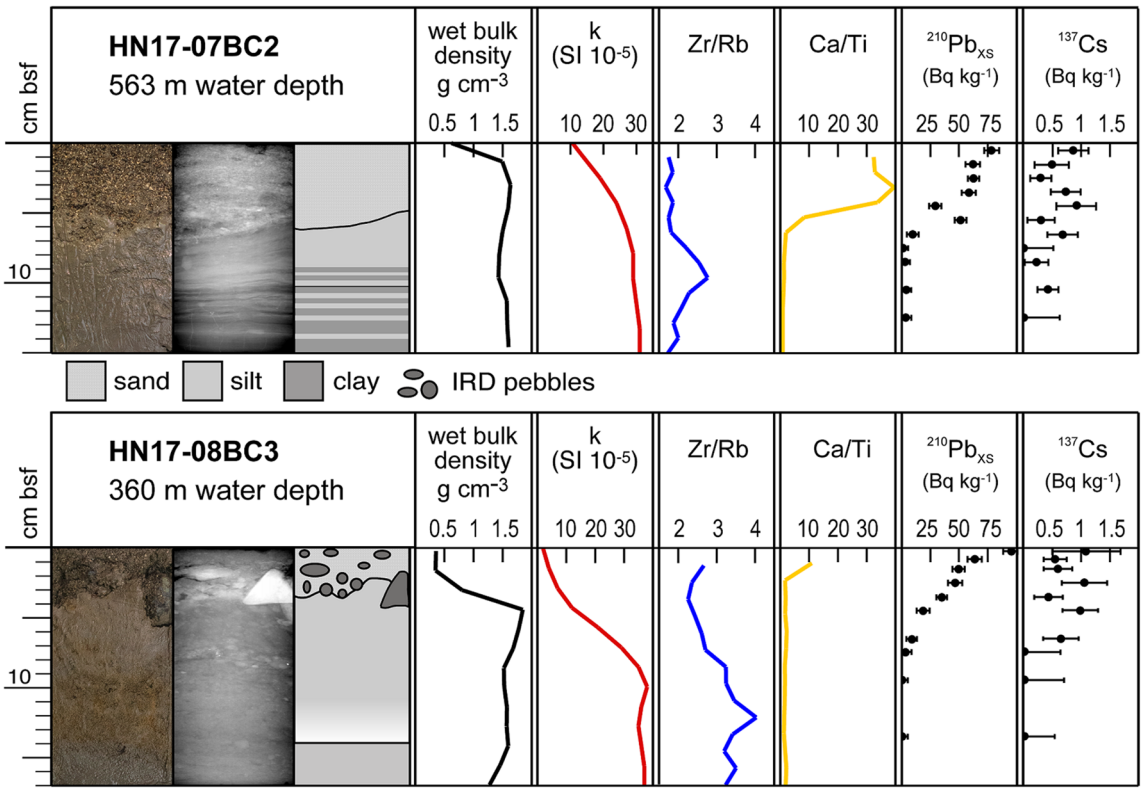

Fig. 4 Photographs, X-radiographs, lithological logs together with graphs of wet bulk density, magnetic susceptibility, Zr/Rb, Ca/Ti, $^{210}Pb_{xs}$ and ^{137}Cs of the two box cores recovered in the INBIS Channel System. Core HN17-07BC2, in a gully on the continental slope, indicates fine-grained turbidites (terrigenous laminations at the core bottom). Core HN17-08BC3, on the outer shelf, indicates the presence of a high-energy environment with condensed sequences (lag deposit at the core top) unaffected by depositional gaps

depth-to-width ratio of the incision is ca. 1/10. The bottom of the gullies is moderately smooth in the area close to the shelf break, with water depths varying between 420 and 750 m, becoming slightly rougher at water depths of ca. 800–900 m (Fig. 6, profile A). Levees are absent in the upper part of the INBIS channel system.

On the shelf west of Bear Island, at a distance of 2 and 5 km from the shelf edge two curved ridges are present (Fig. 2). These ridges are about 2–3 km wide and a few tens of metres high, extending from the Kveithola Trough to the Bear Island Trough for ~ 100 km. These ridges are parallel and close to the shelf break in front of Bear Island, while more to the south they become more distant and more oblique with respect to the shelf break and subparallel to the Bear Island Trough flowlines.

The northern part of the middle slope

The gradient of the middle slope in the northern part of the channel system is ~ 1° to 2° (Fig. 3). This area hosts 23 of the 40 gullies present on the upper reaches. The gullies display symmetrical, V-shaped cross sections (Fig. 5), with a depth/width ratio of ca. 1/10, and variable sinuosity. The gullies converge downslope into larger channels, at water depths of 750–1000 m. At these depths, the channels are characterized by U-shaped cross profiles (Fig. 5) with widths varying between 600 and 2200 m, and incision depths of 30–150 m. Both incision depth and width increase downslope, while the thalweg of the channels become gradually rougher (Fig. 6). The ratio between incision depth and width decreases to around 1/20 with increasing water depth (Fig. 5). The inter-channel width is highly variable, ranging from hundreds of metres to a maximum of about 5 km (Fig. 3). Small levees were observed on the northern flank of some channels. The northernmost of these channels, which marks the northern limit of the INBIS channel system, has the shallowest incision depth (only a few metres), and its profile is highly asymmetric at a water depth of around 1200 m, with a lower gradient on the northern flank (Fig. 5). This channel merges downslope with three channels at a water depth of around 1600 m and eventually reaches the main channel (described further below) at a water depth of around 1820–1850 m (Fig. 3).

The other channels observed in the northern middle slope converge at water depth varying between 1250 and 1600 m

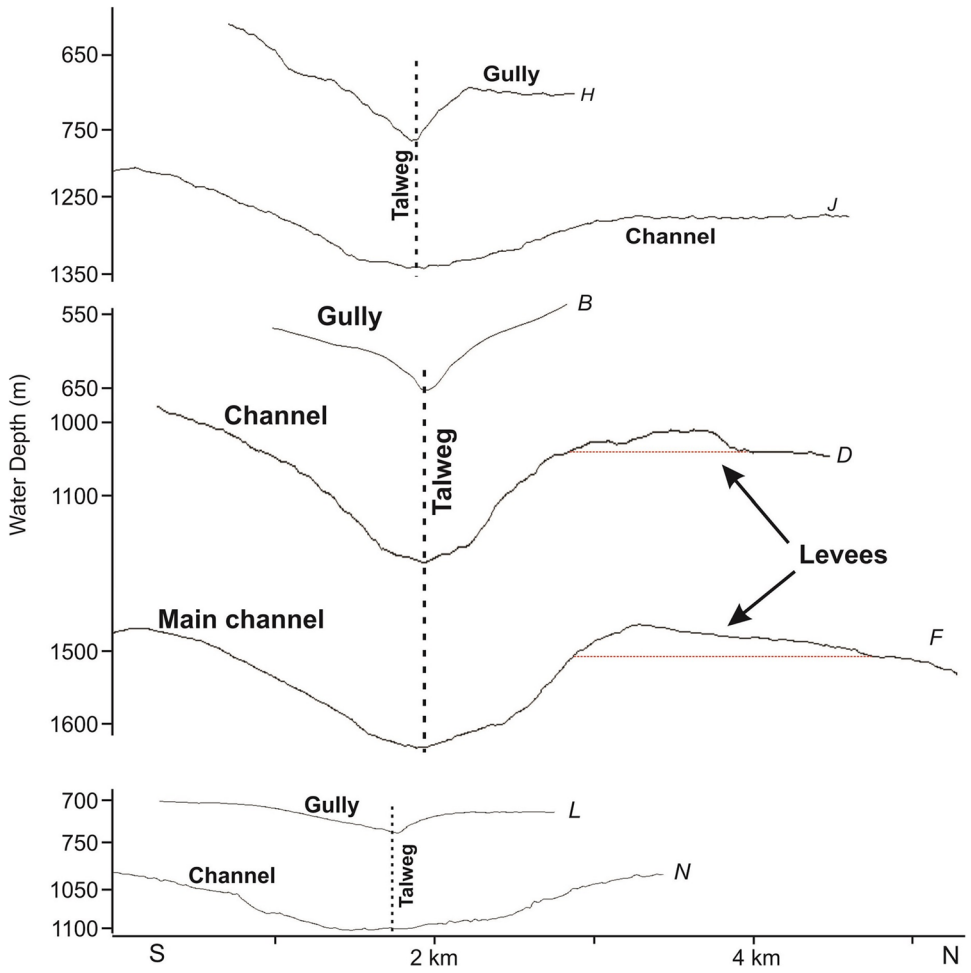

Fig. 5 Bathymetric sections in strike directions (B, D, F, H, J, L and N) of the INBIS Channel System. Location in Fig. 3. Horizontal red dashed lines are to emphasise the relief of the levee deposits

and eventually merge into one at a water depth of around 1600 m.

The main channel (resulting from the merging of the channels in both the northern and southern middle slopes) starts at a water depth of around 1800 m and its axis is E–W oriented. The shallower channel leading to it is about 1000 m wide until around 1850 m water depth (Fig. 3) where its width increases rapidly up to 2500 m and where its incision depth increases from 30 to 150 m (Fig. 3). The surface of the thalweg is relatively flat in the shallower portions of the channel, and becomes increasingly rough in the deeper part (Fig. 6). The cross-channel profiles of the channel are relatively smooth and symmetric in the upper part, while they become progressively more asymmetric below 1150 m water depth, with a steeper gradient characterizing the northern side-wall. At about 1000 m and 1450 m water depth, the northern side-wall of the channel is characterized by ~ 7 m high levees (Fig. 5, profiles D and F), whereas between water depths of 1200 and 1450 m, the channel is bordered to the north by a slightly upward convex sedimentary body, with a variable vertical relief of 5–10 m and a width of about 4 km. The lower part of the Bear Island TMF (Figs. 2, 3) affects the orientation of the main channel around 1800 m water depth, forcing it into a WNW direction.

The southern part of the middle slope

The southern part of the INBIS Channel System extends to a depth of about 1800 m (Fig. 3). The gradient of the slope is, in general, lower with respect to the northern area, with an average slope of about 1°. Here 17 of the gullies observed in the upper reaches converge. The southernmost 5 gullies continue beyond the data coverage, while the remaining 12 gullies merge into three U-shaped channels. The southern one is the most prominent, with a width ranging from 1150 to 2500 m and an incision depth of 40–60 m (Fig. 5, N). The other two channels are slightly smaller, and characterized by widths varying between 900 and 1100 m and incision depths ranging between 30 and 50 m. These two channels partially braid between the water depths of 1450 m and 1700 m (Fig. 3).

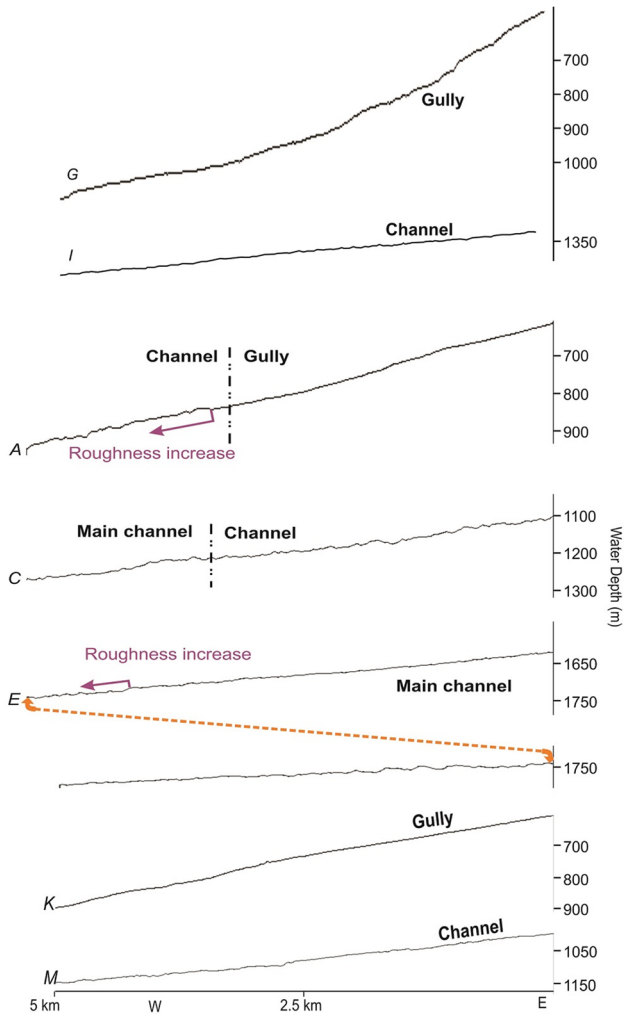

Fig. 6 Bathymetric sections in dip directions (A, C, E, G, I, K and M) of the INBIS channel system. Location in Fig. 3. Profile E (located inside the main channel) is twice as long; the orange dashed line indicates the same point

Sedimentological characteristics and chronology of sub-surface sediments

Core HN17-06BC1 recovered in the southern area of the INBIS Channel System, on the outer shelf close to the southernmost recognized gully (Fig. 3), recovered only a smear of terrigenous/detritic sand with pebbles and cobbles. A first attempt of coring at this site failed to recover any sediment. Hull-mounted acoustic doppler current profiler (ADCP) measurements of the local oceanographic configuration indicated the presence of northward flowing bottom currents on the outer shelf with a speed exceeding 40 cm s^{-1} [35]. The presence of a coarse grained, pebbly substrate combined with strong bottom currents prevented sediment sampling at this site.

Core HN17-07BC2, retrieved from the upper part of the slope (Fig. 3), contains about 6 cm of dark olive grey (Munsell 5y 3/2) fine to medium sand overlying very dark grey (Munsell 5y 3/1) layered silt (6–13 cm bsf) and silty-clay (13–15 cm bsf) sediments. The contact between the upper two lithological units is irregular, possibly erosive. The composition of the uppermost sand is mixed, with the terrigenous fraction mainly composed of rock fragments (detritic till) and the biogenic fraction composed of shelf derived, redeposited bioclasts. The relatively high Ca/Ti ratio and low magnetic susceptibility (Fig. 4) support the presence of bioclast-rich sands in the uppermost 6 cm overlying terrigenous sediments (low Ca/Ti ratio and high magnetic susceptibility). The $^{210}Pb_{xs}$ profile in this core appears affected by mixing in the upper 5–6 cm bsf. as indicated by the relatively constant $^{210}Pb_{xs}$ profile with values around 60 ± 12 Bq kg^{-1}, instead of a typical exponentially down-core decreasing profile. Below 6–7 cm bsf to the core bottom, the mean $^{210}Pb_{xs}$ activity is close to zero (4 ± 3 Bq kg^{-1}), although it never decays to zero value. Such a trend, coherent in both $^{210}Pb_{xs}$ and ^{137}Cs activity profiles, indicates the presence of post-depositional processes acting on the whole sediment core (i.e. biological and/or mechanical mixing such as anthropogenic fishing activity). Therefore, standard $^{210}Pb_{xs}$ dating models are not applicable for this core. However, the presence of $^{210}Pb_{xs}$ through the whole core indicates sediment layers younger than ~ 110 years.

Core HN17-08BC3, recovered on the outer shelf, in the uppermost 4 cm contains coarse sand (Munsell 2.5y 3/2) with scattered pebbles and cobbles overlaying a sharp, irregular base. Between 4 and 14 cm, there is a normally graded interval formed at the base by faintly laminated sand to silt (Munsell 2.5y 4/3) and mottled clayey sediments at the top (Munsell 5y 4/2). The normally graded unit overlays, with a sharp-irregular contact, deeper fine-grained mud sediments located at the base of the core (14–17 cm bsf, Munsell 5y 3/2). The composition of the sands at the top is mainly terrigenous/detritic. The scarce biogenic fraction is mainly of shelf provenance (e.g. bryozoa), with pristine shells of pteropods associated to pelagic deposition. The rest of the sedimentary sequence is terrigenous as also indicated by the very low Ca/Ti ratio and higher magnetic susceptibility. The normally graded interval described between 4 and 14 cm bsf can be also depicted by the trend of the Zr/Rb ratio (Fig. 4). The $^{210}Pb_{xs}$ activity profile in core HN17-08BC3 is characterized by a typical exponentially down-core decrease with a well-defined $^{210}Pb_{xs}$ zero value below 8–9 cm bsf. Applying the CRS dating model, the mean value of Sediment Accumulation Rate (SAR) is 0.06 ± 0.02 cm $year^{-1}$. In this core, the ^{137}Cs down-core profile cannot be used as independent parameter to validate ^{210}Pb dating profile, as ^{137}Cs activities are too close to the minimum detection limit and post-depositional processes cannot be ruled out. For this reason,

the above SAR value should be considered as a maximum. Notwithstanding, the HN17-08BC3 SAR value is in agreement with SAR values determined in the adjacent Kveithola TMF [15].

Discussion

Morphology and depositional areas of the INBIS channel system

On the basis of the slope gradient, we distinguished two main morphological areas in the INBIS channel system that, in turn, are characterized by different depositional processes: the upper reaches, which extends from the shelf break to the upper continental slope, and the middle slope.

In the upper reaches, along the upper slope of the INBIS Channel System, the presence of predominantly V-shaped gullies of similar size and regular spacing, with rarely developed levees, is associated with fast processes of flow bypass and erosion responsible for down-slope sediment transport. The presence in the mid-slope channel area of scarcely developed levees of small dimensions suggests that in this part of the INBIS channel system, downslope sediment transport was restricted to the gullies' thalweg with occasional over spilling. Bypass processes in the area might be related to the density-driven currents as the primary formation mechanism of the INBIS channel (e.g. [85]). Such types of density-driven currents descending the southern flank of the Storfjorden TMF, the northern flank of the Bear Island TMF and the inter-fan area in front of Kveithola TMF were active mainly during glaciations. The origin of these density-driven currents has been previously attributed to dense water formed by cooling and brine rejection during sea-ice formation and/or to turbidity currents generated from small landslides on the upper slope [27, 85].

The gullies grow in dimension down the slope and develop into U-shaped channels (Fig. 5) with progressively increasing rougher bases (Fig. 6). Gully growth might be related to intensification of erosion as a consequence of the gullies/channels coalescence combined with a decrease in slope gradient. In the upper gully-dominated part of the slope, the gradient is up to 5°, with consistent erosive processes determining V-shaped incisions. Further downslope the gradient decreases down to 1°–2° and the gullies evolve into wider, U-shaped channels.

Similar V-shaped gullies on steep TMF slopes in both Arctic (e.g. [77]) and Antarctic (e.g. [55]) continental margins have been related to erosion by gravity-driven processes such as high-energy, dense subglacial meltwaters occurring during deglaciation (e.g. [29, 49, 50, 52]).

However, meltwaters are not the only flows that may have contributed to the formation of this upslope part of the INBIS channel system. During glacial maxima, sediments accumulate beyond the shelf edge, transported and deposited by the ice streams. The collapse of these glacigenic sediment accumulations produces debris flows (e.g. [42–44, 85]). The INBIS Channel is marginally infilled by glacigenic debris flows, which were most abundant during glacial maxima [42].

We infer that the two curved ridges at 2 and 5 km from the shelf edge (Fig. 2) described in Sect. "The upper reaches of the INBIS channel system" are shelf-edge moraines, subglacial landforms located in areas of slow-moving ice, similar to those observed west of the Lofoten Islands on the western Norwegian margin [9, 10, 87]. Another hypothesis is that these ridges are margin moraines formed in the transition zones between fast-flowing ice (ice streams) and slower-flowing ice (or absence of ice), similar to those observed in the Vestfjorden Trough by Ottesen et al. [61].

In the middle slope of the INBIS channel system, from about 1000 m water depth, the gullies merge into channels. The flows originating the upper-slope gullies are funnelled through the centre of the area, and as a consequence the larger channel forms. We infer that the merging of a large number of gullies into fewer channels along with the gradient decrease may cause changes in the nature of the flows, causing irregular erosion, similar to that observed in the Kongsfjorden Channel System by Forwick et al. [27]. As a consequence, in the deeper part of these channels, the bottom roughness increases. Also the appearance of levees suggests that the energy of the flows is sufficient to overtop the channel flanks.

Most of the other gullies/channels eventually converge downslope, and several processes probably led to the asymmetry of the flanks here. First, due to the decreasing energy of the flows as a consequence of lower slope gradient, the finest component of the sediment load is delayed and deflected to the right by the Coriolis force. This produces overbank accumulations (levees) on the right (northern) flank of the main channel, similar to those reported for the lower INBIS Channel by Vorren et al. [85]. Second, the northward-flowing West Spitsbergen Current (WSC) may prevent sediments from settling on the southern side of the channels in this part of the INBIS channel system, supporting deflection of the suspended sediment to the right of the channel and the deposition of sediments on the northern side.

Reconstruction of the geological history of the INBIS channel system

The morphogenetic analysis of the INBIS channel system led to the identification of two main domains that have undergone different geological evolution.

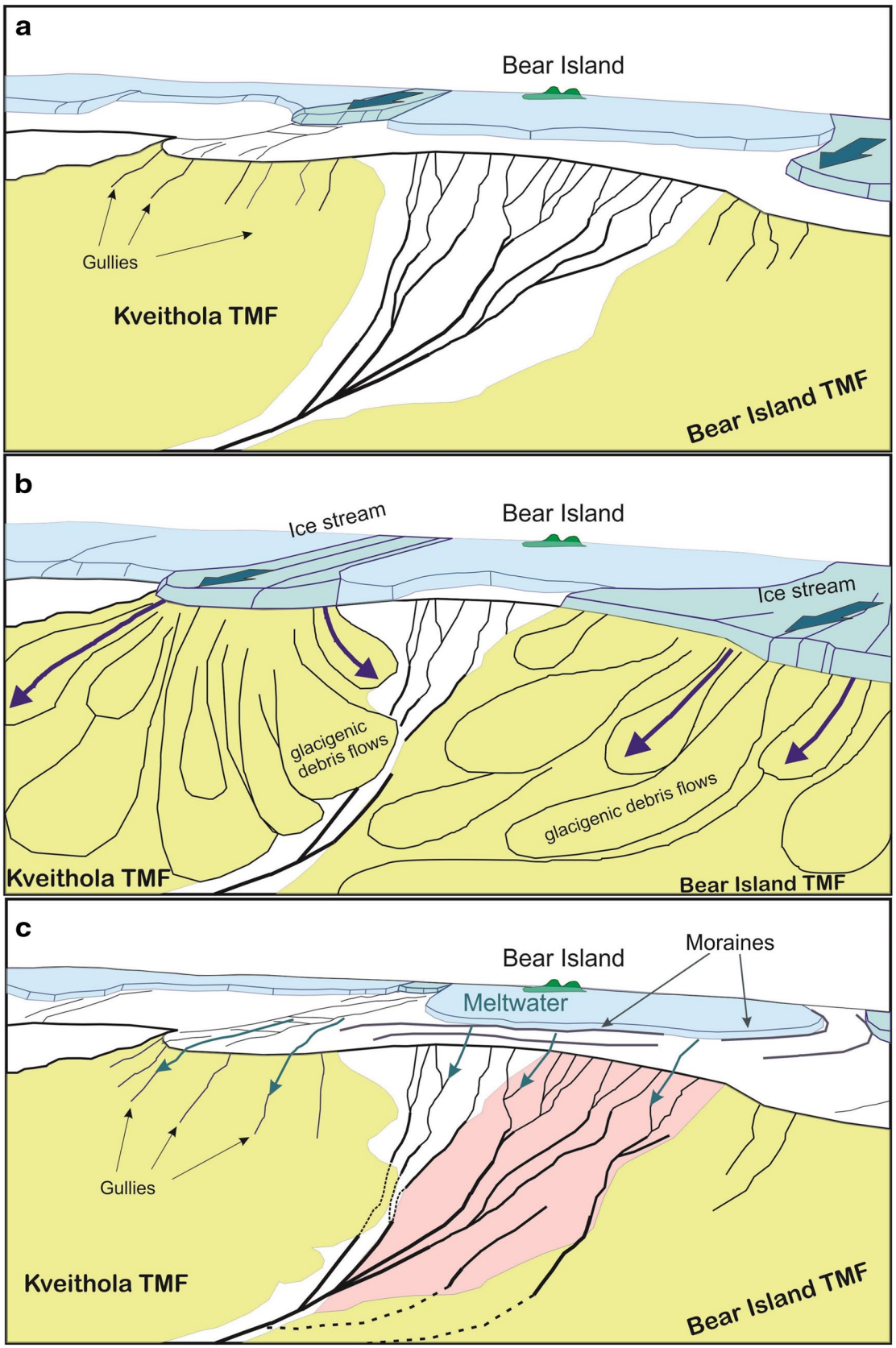

◂**Fig. 7** Schemes of inferred pre-LGM state (**a**), LGM state (**b**) and post-LGM state (**c**) of the INBIS Channel System. Green arrows indicate the location and direction of area of fast-moving ice (ice streams, slightly darker than the rest of the ice sheet). Downslope, the gullies (thin black lines) merge and evolve into channels (thick black lines). Blue arrows (**b**) indicate the direction of glacigenic debris flows, forming depositional lobes on both Kveithola and Bear Island TMF (in yellow). During the ice sheet retreat (**c**) meltwaters (light blue) flow downslope past the shelf edge, both in the INBIS Channel System and in the Kveithola and Bear Island TMFs (in yellow). Meltwaters carve new gullies into the glacigenic debris flow deposits in the southern part of the INBIS channel system (pink area) and on the TMFs (see **b** for comparison). Shelf-edge moraines (labelled in grey) mark the maximum extent of the ice sheet around Bear Island

The Northern area (northern upper reaches and slope), characterized by sharp/pristine erosive structures, is the area that possibly never experienced the arrival of massive, glacigenic debris flows. Such a type of morphology can instead be compared with the canyon systems that typically dissect mid- and low-latitude margins (e.g. Hudson Trough, [54]) derived from river-incision on shelf sediments and erosion during low sea-level stands, associated turbidity flows, and internal tide waves/currents. We believe the Northern area of the INBIS Channel System developed through the funnelling of low-medium density flows, i.e.: turbidity currents [26] delivered during glacial times and early deglaciation; and plumes linked to the release of meltwaters derived from basal glacial melting and retreat [22, 48, 50, 55, 92]; currents related to high salinity cold waters (brine) originating from rejection during sea-ice formation (the latter process was already suggested by Vorren et al. [85]). Furthermore, Fohrmann et al. [26] indicated that consistent slope erosion presently occurs by means of mixed brine and suspended bottom sediments that generate powerful turbidity currents (the so-called TS turbidites). In support to this, we found evidence of turbidity currents and deposition in the studied upper slope cores HN17-07BC2 (laminated sediments), and core HN17-08BC3 (normally graded deposits). In agreement with the sedimentary facies described along the neighbouring Kveithola outer trough [47], the shelf edge of the INBIS Channel area appears presently swept by strong bottom currents (possibly the northwards flowing West Spitsbergen Current). Such currents are responsible for deposition of the medium-grained sands and pebbles lag deposit recovered at the top of cores HN17-07BC2 and HN17-08BC3, possibly preventing sampling at site HN17-06BC1. This is supported also by the very low-mean Sediment Accumulation Rate (0.06 ± 0.02 cm year^{-1}), calculated at station HN17-08BC3 for the last century.

Similar to the diversion of ice around topographic highs observed by Knight et al. [40] on the Greenland ice sheet, we infer that the advances of the ice sheet, and in particular, the ice streams in the studied area were partially diverted by the presence of Bear Island, preventing the formation of a continuum between the Kveithola and the Bear Island TMFs. It is plausible that a local ice cap around Bear Island had already developed before the surrounding ice streams reached the shelf break. We infer that when the SBKIS reached this part of the margin, Bear Island worked as a pin (fastener) for the surrounding ice. The fast ice streams of Bear Island and Kveithola diverged around Bear Island and flowed in the troughs (e.g. [21, 39, 50, 69, 70]) (Fig. 7b), creating west of Bear Island an inter-ice stream region of slower-flowing ice. We infer that the maximum extent of the local ice cap around Bear Island is marked by the outermost of the ridges described in "The upper reaches of the INBIS channel system" (Figs. 2, 7c).

The hypothesis that the SBKIS did not reach the shelf edge in this part of the margin is further supported by the conceptual model of slope sedimentation on glacier-influenced continental margin of Dowdeswell et al. [20, their Fig. 25; [19, 67]. The elements constraining the model are the proximity of the ice sheet/stream to the shelf edge, the sediment input and the type of sedimentary products. A glacier-influenced margin is divided in three types: (1) sediment starved margin, characterized by an ice sheet not reaching the shelf edge, low sediment input and the formation of submarine channels; (2) inter-fan area, characterized by an ice sheet reaching the shelf edge, moderate sediment input and the formation of mass transport deposits; (3) trough mouth fan (TMF), characterized by an ice-stream reaching the shelf edge, the highest sediment input and the formation of debris flow deposits. Although the INBIS Channel System is located in an inter-fan area, where the inter-ice stream part of the ice sheet could potentially reach the shelf edge, the slope is not characterized by landslide scars or landslide deposits, which are distinctive characteristics of the slopes in inter-fan area on a glacier-influenced margin (e.g. 51, 60, 65]). On the contrary, the formation of a submarine channel system is a characteristic of a sediment starved margin, i.e. a part of the margin where the ice sheet did not reach the shelf edge (e.g. Kaiser Franz Joseph Fjord, East Greenland, [89, 25]). We therefore infer that this part of the continental margin is a special case of an inter-fan sediment starved area: the reduced amount of sediment input is to be attributed to the slower-flowing ice not reaching the shelf edge due to the presence of Bear Island. This hypothesis matches with the updated version of the model of glacier-influenced continental margin presented by Pope et al. [67]. In this schematic model, channel systems are expected to develop in between glacial troughs in low sediment input margins (e.g. Fig. 28 in [67]). Another example of channel formed in a sediment-starved margin can be found on the continental slope north of Nordaustlandet (Svalbard) in front of the Albertini Trough [28]. In this part of the margin, there is large accommodation space for sedimentation below the outer Albertini Trough due to down-faulted bedrock. Therefore, the glacigenic

sediments transported by ice streaming through the Albertini Trough accumulated in the accommodation space of the outer-shelf basin, preventing the formation of a TMF and allowing the formation of a submarine channel [28].

The Southern area (southern upper reaches and slope) is characterized by smoothed erosive structures that according to the morphological analysis, suggest the presence of relict mass transport deposits crossing the upper slope with a SE–NW orientation (Fig. 7b, c). We argue that these mass transport deposits did not originate on the slope as submarine landslides and they might actually represent glacigenic debris flows delivered to the southern INBIS channel system area by the northern fringe of the Bear Island ice stream during past glacial maxima. The morphological evidences supporting this hypothesis include: a remarkably lower gradient of the upper slope (about 1° versus up to 5° of the Northern area) that is comparable to the neighbouring TMF, with deeper location of the gradient change between the upper and middle slopes (1100 m water depth instead than 700 m water depth in the Northern area); the reduced incision depth of the gullies (10 m depth) with respect to the northern area (60 m depth); a reduced number of secondary channels on the middle slope that are characterized by a relatively small height/width ratio (1/20 instead of 1/10 of the Northern area).

According to the morphologies observed on the INBIS channel and surrounding areas, we infer that such glacigenic debris flows must have been emplaced on the slope earlier than the Middle Weichselian glaciation. We argue that the southern channels might have been carved on high-density glacigenic debris flows, resulting in a less pronounced shape than the channels observed in the Northern area of the INBIS channel system. Nevertheless, the channels are clearly marked on the sea floor, whereas on the neighbouring TMF systems, that received glacigenic debris flows during LGM, the gullies of the upper slope never developed as proper channels after the LGM (see [65]).

Similar glacial dynamics were possibly responsible for the emplacement of the glacial debris flows observed on the middle slope of the Northern area of the INBIS channel system. We infer that glacigenic debris flows from the Kveithola Trough never reached the upper reaches of the INBIS channel system (presence of sharp pristine morphologies), but they only partially invaded the middle slope, burying some of the former channels that appear less pronounced or almost completely obliterated, as seen on the bathymetry (Figs. 3, 7c).

Beside of the relatively recent glacigenic history of the margin attaining to the present INBIS channel system, another hypothesis could explain the formation of a channel system in this inter-TMF area. As a matter of fact, we cannot exclude the possibility that the initial onset of this channel system pre-dates the beginning of glacial conditions. This system could in fact have been the deeper extension of a river system associated with the main sub-aerial relief of Bear Island. The presence of an east–west oriented system of rivers transporting sediments to the margin of the NW Barents Sea has been previously envisaged for the period preceding about 2 Ma by Hjelstuen et al. [32].

Conclusions

In this paper, we presented a morphological description of the upper slope area of the INBIS channel system based on newly acquired bathymetric data. We discussed its genesis and evolution during glacial maxima as well as at present time, its interactions with the TMF systems and its role in sediment drainage to the deeper environment on the west Spitsbergen margin.

- We identified 40 V-shaped gullies dissecting the shelf edge that increase in size downslope, merging with adjacent gullies and evolving into larger U-shaped secondary channels. Secondary channels merge downslope into the main INBIS channel due to lateral confinement by the fringes of the Kveithola and Bear Island TMFs.
- Two morphodynamic areas were distinguished within the INBIS channel system characterized by different geological evolution and drainage system: the Northern area representing a special case of inter-fan, sediment starving margin, and the Southern areas with a more typically inter-fan related sedimentation.
- The shelf break of the Northern area never experienced the massive arrival of glacigenic debris, preserving its original morphologies over the past glaciations. Only the middle slope was affected by the emplacement of glacial debris flows as part of the Kveithola TMF.
- The peculiarity of the continental margin attaining to the INBIS channel system was attributed to the formation, during the past glaciations, of slower-flowing ice associated to the presence of the Bear Island that acts as a pin for the surrounding ice.
- After the onset of glaciations, the system was maintained through time by meltwater release during the ice sheet retreat/decay, and by the erosive effect of brine and other dense gravity currents presently forming on the shelf (TS turbidities) as recorded in sub-surface sediment cores.

Acknowledgements This research was supported by the Italian projects PNRA-EDIPO, the project PNRA-CORIBAR, the rewarding funding project ARCA and the project High North 17, and Spanish projects DEGLABAR (CTM2010-17386) and CORIBAR-ES (CTM2011-14807-E), funded by the Spanish Ministerio de Economía y Competitividad and the European Regional Development Fund.

Compliance with ethical standards

Conflict of interest On behalf of all authors, the corresponding author states that there are no conflicts of interest.

References

1. Amblas D, Canals M, Urgeles R, Lastras G, Liquete C, Hughes-Clarke JE, Casamor JL, Calafat AM (2006) Morphogenetic mesoscale analysis of the northeastern Iberian margin, NW Mediterranean Basin. Mar Geol 234:3–20
2. Amblas D, Gerber TP, De Mol B, Urgeles R, Garcia-Castellanos D, Canals M, Pratson LF, Robb N, Canning J (2012) Survival of a submarine canyon during long-term outbuilding of a continental margin. Geology 40:543–546
3. Amundsen HB, Laberg JS, Vorren TO, Haflidason H, Forwick M, Buhl-Mortensen P (2015) Late Weichselian—Holocene evolution of the high-latitude Andøya submarine canyon, North-Norwegian continental margin. Mar Geol 363:1–14
4. Andreassen K, Winsborrow M, Bjarnadóttir L, Rüther D, Borque J, Lucchi R, Caburlotto A (2009) Barents Sea and the West Spitsbergen Margin, UiT 2009. Marine Geophysical/Geological Cruise to Outer Bear Island trough, Kveithola trough and the West Spitsbergen Margin, Cruise Report. RV/Jan Mayen 2.-19.07.2009 University of Tromsø, p 33
5. Andreassen K, Winsborrow MCM, Bjarnadóttir LR, Rüther DC (2014) Ice stream retreat dynamics inferred from an assemblage of landforms in the northern Barents Sea. Quat Sci Rev 92:246–257
6. Andreassen K, Bjarnadóttir LR, Rüther DC, Winsborrow MCM (2016) Retreat patterns and dynamics of the former Bear Island Trough Ice stream. Geol Soc Lond Mem 46:445–452
7. Appleby PG, Oldfield F (1978) The calculation of lead-210 dates assuming a constant rate of supply of unsupported 210Pb to the sediment. Catena 5:1–8
8. Appleby PG (1979) 210Pb dating of annually laminated lake sediment from Finland. Nature 280:53–55
9. Batchelor CL, Dowdeswell JA (2015) Ice-sheet grounding-zone wedges (GZWs) on high-latitude continental margins. Mar Geol 363:65–92
10. Batchelor CL, Dowdeswell JA, Ottensen D (2017) Submarine glacial landforms. In: Micallef A, Krastel S, Savini A (eds) Submarine geomorphology. Springer geology, Springer, Cham, Switzerland, pp 207–234
11. Bjarnadóttir LR, Rüther DC, Winsborrow MCM, Andreassen K (2013) Grounding-line dynamics during the last deglaciation of Kveithola, W Barents Sea, as revealed by seabed geomorphology and shallow seismic stratigraphy. Boreas 42:84–107
12. Bjarnadóttir LR, Winsborrow MCM, Andreassen K (2017) Large subglacial meltwater features in the central Barents Sea. Geology 45:159–162
13. Camerlenghi A, Flores JA, Sierro FJ, Colmenreo E, the SVAIS Scientific and Tchnical Staff (2007) SVAIS, the Development of an Ice Stream-dominated Sedimentary System: the Southern Svalbard Continental Margin. University of Barcelona, Cruise report, p 62
14. Canals M, Casamor JL, Lastras G, Monaco A, Acosta YJ, Berne S, Loubrieu B, Weaver P, Greham A, Dennielou B (2004) The role of Canyons in strata formation. Oceanography (Washington, DC) 17:80–91
15. Caricchi C, Lucchi RG, Sagnotti L, Macrì P, Morigi C, Melis R, Caffau M, Rebesco M, Hanebuth TJJ (2018) Paleomagnetism and rock magnetism from sediments along a continental shelf-to-slope transect in the NW Barents Sea: Implications for geomagnetic and depositional changes during the past 15 thousand years. Glob Planet Change 160:10–27
16. Carroll J, Lerche I (2003) Sedimentary processes: quantification using radionuclides. Elsevier, Oxford
17. Croudace IW, Rindby A, Guy Rothwell RG (2006) ITRAX: description and evaluation of a new multi-function X-ray core scanner. Geol Soc Spec Publ Lond 267:51–63
18. Delbono I, Barsanti M, Schirone A, Conte F, Delfanti R (2016) 210Pb mass accumulation rates in the depositional area of the Magra River (Mediterranean Sea, Italy). Cont Shelf Res 124:35–48
19. Dowdeswell JA, Kenyon N, Elverhoi A, Laberg JS, Mienert J, Siegert MJ (1996) Large-scale sedimentation on the glacier-influenced Polar North Atlantic margins: long range side-scan sonar evidence. Geophys Res Lett 23:3535–3538
20. Dowdeswell JA, Elverhøi A, Spielhagen R (1998) Glacimarine sedimentary processes and facies on the Polar North Atlantic Margins. Quat Sci Rev 17:243–272
21. Dowdeswell JA, Ó Cofaigh C, Taylor J, Kenyon NH, Mienert J, Wilken M (2002) On the architecture of high-latitude continental margins: the influence of ice-sheet and sea-ice processes in the Polar North Atlantic. In: Dowdeswell JA, ÓCofaigh C (eds) Glacier-Influenced Sedimentation on High-Latitude Continental Margins. Geological Society Special Publications, London, vol 203, pp 33–54
22. Dowdeswell JA, Evans J, Cofaigh C, Anderson JB (2006) Morphology and sedimentary processes on the continental slope of Pine Island Bay, Amundsen Sea, West Antarctic. Geol Soc Am Bull 118(5/6):606–619
23. Dowdeswell JA, Bamber JL (2007) Keel depths of modern Antarctic icebergs and implications for sea-floor scouring in the geological record. Mar Geol 243:120–131
24. Elverhøi A, Andersen ES, Dokken T, Hebbeln D, Spielhagen R, Svendsen JI, Sorflaten M, Rornes A, Hald M, Forsberg CF (1995) The growth and decay of the late Weichselian ice sheet in western Svalbard and adjacent areas based on provenance studies of marine sediments. Quat Res 44:303–316
25. Elverhøi A, Dowdeswell JA, Funder S, Mangerud J, Stein R (1998) Glacial and oceanic history of the polar north Atlantic margins: an overview. Quat Sci Rev 17:1–10
26. Fohrmann H, Backhaus JO, Blaume F, Rumohr J (1998) Sediments in bottom-arrested gravity plumes: Numerical case studies. J Phys Oceanogr 28:2250–2274
27. Forwick M, Laberg JS, Hass HC, Osti G (2015) The Kongsfjorden channel system offshore NW Svalbard: downslope sedimentary processes in a contour-current-dominated setting. Arktos 1:1
28. Fransner O, Noormets R, Flink AE, Hogan KA, Dowdeswell JA (2018) Sedimentary processes on the continental slope off Kvitøya and Albertini troughs north of Nordaustlandet, Svalbard—the importance of structural-geological setting in trough-mouth fan development. Mar Geol 402:194–208
29. Gales JA, Forwick M, Laberg JS, Vorren TO, Larter RD, Graham AGC, Baeten NJ, Amundsen HB (2013) Arctic and Antarctic submarine gullies—a comparison of high latitude continental margins. Geomorphology 201:449–461
30. García M, Batchelor CL, Dowdeswell JA, Hogan KA, Cofaigh Ó (2016) A glacier-influenced turbidite system and associated landform assemblage in the Greenland Basin and adjacent continental slope. In: Dowdeswell JA, Canals M, Jackobbson M, Todd BJ, Dowdeswell EK, Hogan KA (eds) Atlas of submarine glacial landforms: modern, quaternary and ancient. Geological Society, London, Memoirs, vol 46, pp 461–468
31. Harris PT, Whiteway T (2011) Global distribution of large submarine canyons: geomorphic differences between active and passive continental margins. Mar Geol 285:69–86

32. Hjelstuen BO, Elverhøi A, Faleide JI (1996) Cenozoic erosion and sediment yield in the drainage area of the Storfjorden Fan. Glob Planet Change 12:95–117
33. Hughes ALC, Gyllencreutz R, Lohne ØS, Mangerud J, Svendsen JI (2016) The last Eurasian ice sheets—a chronological database and time-slice reconstruction, DATED-1. Boreas 45:1–45
34. Hyvärinen H (1968) Late-Quaternary sediment cores from lakes on Bjørnøya. Geogr Ann 50:235–245
35. Ivaldi R, Demarte M, HIGH NORTH 17 Team (2017) HIGH NORTH 17 cruise report, Istituto Idrografico della Marina, pp 1–70
36. Jakobsson M et al (2012) The international bathymetric chart of the Arctic Ocean (IBCAO) Version 3.0. Geophys Res Lett 39:12
37. Jessen SP, Rasmussen TL, Nielsen T, Solheim A (2010) A new Late Weichselian and Holocene marine chronology for the western Svalbard slope 30,000-0 cal years BP. Quat Sci Rev 29:1301–1312
38. Jones GA, Keigwin LD (1988) Age determinations on sediment core PS1295-4, Supplement to Jones GA, Keigwin LD, 1988. Evidence from Fram Strait (78°N) for early deglaciation. Nature 336(6194):56–59
39. Knies J, Vogt C, Stein R (1999) Late Quaternary growth and decay of the Svalbard/Barents Sea ice sheet and paleoceanographic evolution in the adjacent Arctic Ocean. Geo-Mar Lett 18:195–202
40. Knight P, Sugden D, Minty C (1994) Ice flow around large obstacles as indicated by basal ice exposed at the margin of the Greenland ice sheet. J Glaciol 40(135):359–367
41. Koide M, Soutar A, Goldberg ED (1972) Marine geochronology with 210Pb. Earth Planet Sci Lett 14:442–446
42. Laberg JS, Vorren TO (1995) Late Weichselian submarine debris flow deposits on the Bear Island Trough Mouth Fan. Mar Geol 127(1–4):45–72
43. Laberg JS, Vorren TO (1996) The middle and late pleistocene evolution of the Bear Island Trough Mouth Fan. Glob Planet Change 12:309–330
44. Laberg JS, Vorren TO (2000) Flow behaviour of the submarine glacigenic debris flows on the Bear Island Trough Mouth Fan, western Barents Sea. Sedimentology 47:1105–1117
45. Laberg JS, Guidard S, Mienert J, Vorren TO, Haflidason H, Nygård A (2007) Morphology and morphogenesis of a high-latitude canyon; the Andøya Canyon, Norwegian Sea. Mar Geol 246:68–85
46. Landvik JY, Bondevik S, Elverhøi A, Fjeldskaar W, Mangerud J, Salvigsen O, Siegert MJ, Svendsen JI, Vorren TO (1998) The last glacial maximum of Svalbard and the Barents Sea area: ice sheet extent and configuration. Quat Sci Rev 17:43–75
47. Lantzsch H, Hanebuth TJJ, Horry J, Grave M, Rebesco M, Schwenk T (2017) Deglacial to Holocene history of ice-sheet retreat and bottom current strength on the western Barents Sea shelf. Quat Sci Rev 173:40–57
48. Llopart J, Urgeles R, Camerlenghi A, Lucchi RG, De Mol B, Rebesco M, Pedrosa MT (2016) Slope instability of glaciated continental margins: Constraints from permeability-compressibility tests and hydrogeological modelling off Storfjorden, NW Barents Sea. In: Submarine Mass Movements and Their Consequences, 6th International Symposium, pp 95–104
49. Lucchi RG, Pedrosa MT, Camerlenghi A, Urgeles R, De Mol B, Rebesco M (2012) Recent submarine landslides on the continental slope of Storfjorden and Kveithola Trough-Mouth Fans (north west Barents Sea). In: Yamada Y, Kawamura K, Ikehara K, Ogawa Y, Urgeles R, Mosher D, Chaytor J, Strasser M (eds) Submarine mass movements and their consequences. Advances in natural and technological hazards research. Springer Science Book Series, Berlin, vol 31, pp 735–745
50. Lucchi RG, Camerlenghi A, Rebesco M, Urgeles R, Sagnotti L, Macri P, Colmenero- Hildago E, Sierro FJ, Melis R, Morigi C, Barcena MA, Giorgetti G, Villa G, Persico D, Flores JA, Pedrosa MT, Caburlotto A (2013) Postglacial sedimentary processes on the Storfjorden and Kveithola trough-mouth fans: impact of extreme glacimarine sedimentation. Glob Planet Change 111:309–326
51. Madrussani G, Rossi G, Rebesco M, Picotti S, Urgeles R, Llopart J (2018) Sediment properties in submarine mass-transport deposits using seismic and rock-physics off NW Barents Sea. Mar Geol 402:264–278
52. Melis R, Carbonara K, Villa G, Morigi C, Bárcena MA, Giorgetti G, Caburlotto A, Rebesco M, Lucchi RG (2018) A new multiproxy investigation of Late Quaternary palaeoenvironments along the north-western Barents Sea (Storfjorden Trough Mouth Fan). J Quat Sci 33:662–676
53. Mienert J, Kenyon NH, Thiede J, Holender F-J (1993) Polar continental margins: studies off East Greenland. EOS Trans Am Geophys Union 74:225–236
54. Mosher DC, Campbell DC, Gardner JV, Piper DJW, Chaytor JD, Rebesco M (2017) The role of deep-water sedimentary processes in shaping a continental margin: the Northwest Atlantic. Mar Geol 393:245–259
55. Noormets R, Dowdeswell JA, Larter RD, Cofaigh C, Evans J (2009) Morphology of the upper continental slope in the Bellingshausen and Amundsen Seas—implications for sedimentary processes at the shelf edge of West Antarctica. Mar Geol 258:100–114
56. Normark WR, Posamentier H, Mutti E (1993) Turbidite systems: state of the art and future directions. Rev Geophys V 31:91–116
57. Normark WR, Carlson PR (2003) Giant submarine canyons: is size any clue to their importance in the rock record? In: Chan MA, Archer AW (eds) Extreme depositional environments: mega end members in geologic time, vol 370. Geological Society of America, Boulder, USA, pp 175–190
58. Ò Cofaigh C, Dowdeswell JA et al (2004) Timing and significance of glacially influenced mass-wasting in the submarine channels of the Greenland Basin. Mar Geol 207:39–54
59. Ò Cofaigh C, Andrews JT, Jennings AE, Dowdeswell JA, Hogan KA, Kilfeather AA, Sheldon C (2013) Glacimarine lithofacies, provenance and depositional processes on a West Greenland trough-mouth fan. J Quat Sci 28:13–26
60. O'Grady DB, Syvitsky JPM (2002) Large-scale morphology of Arctic continental slopes: the influence of sediment delivery on slope form. Geological Society Special Publications, London, vol 203, pp 11–31
61. Ottesen D, Rise L, Knies J, Olsen L, Henriksen S (2005) The Vestfjorden-Trænadjupet palaeo-ice stream drainage system, mid-Norwegian continental shelf. Mar Geol 218:175–189
62. Patton H, Andreassen K, Bjarnadóttir LR, Dowdeswell JA, Winsborrow CM, Noormets R, Polyak L, Auriac A, Hubbard A (2015) Geophysical constraints on the dynamics and retreat of the Barents Sea Ice sheet as a palaeo-benchmark for models of marine ice-sheet deglaciation. Rev Geophys 53:1051–1098
63. Patton H, Hubbard AL, Andreassen K, Auriac A, Whitehouse PL, Stroeven AP, Shackleton C, Winsborrow MCM, Heyman J, Hall AM (2017) Deglaciation of the Eurasian ice sheet complex. Quat Sci Rev 169:148–172 (**ISSN 0277–3791**)
64. Peakall J, Kane AI, Masson DG, Keevil G, McCaffrey W, Corney R (2012) Global (latitudinal) variation in submarine channel sinuosity. Geology 40:11–14
65. Pedrosa MT, Camerlenghi A, De Mol B, Urgeles R, Rebesco M, Lucchi RG (2011) Seabed morphology and shallow sedimentary structure of the Storfjorden and Kveithola trough-mouth fans (North West Barents Sea). Mar Geol 286:65–81
66. Petrini M, Colleoni F, Kirchner N, Hughes ALC, Camerlenghi A, Rebesco M, Lucchi RG, Forte E, Colucci RR, Noormets R (2018) Interplay of grounding-line dynamics and sub-shelf melting during retreat of the Bjørnøyrenna Ice Stream. Sci Rep 8:7196

67. Pope EL, Talling PJ, Ò Cofaigh C (2018) The relationship between ice sheets and submarine mass movements in the Nordic Seas during the Quaternary. Earth Sci Rev 178:208–256
68. Rasmussen T, Thomsen E, Ślubowska AM, Jessen S, Solheim A, Koc N (2007) Paleoceanographic evolution of the SW Svalbard margin (76°N) since 20,000 14C yr BP. Quat Res 67:100–114
69. Rebesco M, Liu Y, Camerlenghi A, Winsborrow M, Laberg JS, Caburlotto A, Diviacco P, Accettella D, Sauli C, Wardell N, Tomini I (2011) Deglaciation of the western margin of the Barents Sea Ice Sheet—a swath bathymetric and sub-bottom seismic study from the Kveithola Trough. Mar Geol 279:141–147
70. Rebesco M, Laberg JS, Pedrosa MT, Camerlenghi A, Lucchi RG, Zgur F, Wardell N (2014) Onset and growth of Trough-Mouth Fans on the North-Western Barents Sea margin—implications for the evolution of the Barents Sea/Svalbard Ice Sheet. Quat Sci Rev 92:227–234
71. Rebesco M, Özmaral A, Urgeles R, Accettella D, Lucchi RG, Rüther D, Winsborrow M, Llopart J, Caburlotto A, Lantzsch H, Hanebuth TJJ (2016) Evolution of a high-latitude sediment drift inside a glacially-carved trough based on high-resolution seismic stratigraphy (Kveithola, NW Barents Sea). Quat Sci Rev 147:178–193
72. Rise L, Bøe R, Riis F, Bellec VK, Laberg JS, Eidvin T, Elvenes S, Thorsnes T (2013) The Lofoten-Vesterålen continental margin, North Norway: canyons and mass-movement activity. Mar Pet Geol 45:134–149
73. Robbins JA, Edgington DN (1975) Determination of recent sedimentation rates in Lake Michigan using Pb-210 and Cs-137. Geochim Cosmochim Acta 39:285–304
74. Robbins JA, Edgington DN, Kemp ALW (1978) Comparative 210Pb, 137Cs, and pollen geochronologies of sediments from Lakes Ontario and Erie. Quat Res 10:256–278
75. Rüther DC, Mattingsdal R, Andreassen K, Forwick M, Husum K (2011) Seismic architecture and sedimentology of a major grounding zone system deposited by the Bjørnøyrenna Ice Stream during Late Weichselian deglaciation. Quat Sci Rev 30:2776–2792
76. Rüther DC, Bjarnadóttir LR, Junttila J, Husum K, Rasmussen TL, Lucchi RG, Andreassen K (2012) Pattern and timing of the northwestern Barents Sea Ice Sheet deglaciation and indications of episodic Holocene deposition. Boreas 41:1–19
77. Rydningen TA, Laberg JS, Kolstad V (2015) Seabed morphology and sedimentary processes on high-gradient trough mouth fans offshore Troms, northern Norway. Geomorphology 246:205–219
78. Salvigsen O, Slettemark O (1995) Past glaciation and sea levels on Bjørnøya, Svalbard. Polar Res 14:245–251
79. Sanchez-Cabeza JA, Ruiz-Fernández AC (2012) 210Pb sediment radiochronology: an integrated formulation and classification of dating models. Geochim Cosmochim Acta 82:183–200
80. Shepard FP, Emery KO, (1941) Submarine topography off the california coast: canyons and tectonic interpretations. Geol Soc Am Spec Paper 31:171
81. Smith JN (2001) Why should we believe 210Pb sediment geochronologies? J Environ Radioact 55:121–123
82. Stokes CR, Clark CD (2001) Paleo-ice streams. Quatern Sci Rev 20(13):1437–1457
83. Vorren TO, Lebesbye E, Andreassen K, Larsen KB (1989) Glacigenic sediments on a passive continental margin as exemplified by the Barents Sea. Mar Geol 85:251–272
84. Vorren TO, Laberg JS (1996) Late glacial air temperature, oceanographic and ice sheet interactions in the southern Barents Sea region. In: Andrews JT, Austin WEN, Bergsten H, Jennings AE (eds) Late quaternary palaeoceanography of the north atlantic margins, vol 111. Geological Society, Special Publication, London, pp 303–321
85. Vorren TO, Laberg JS, Blaume F, Dowdeswell JA, Kenyoh NH, Mienert J, Rumohr J, Werner F (1998) The Norwegian-Greenland sea continental margins: morphology and late quaternary sedimentary processes and environment. Quat Sci Rev 17:273–302
86. Vorren TO, Laberg JS (2001) Late Quaternary sedimentary processes and environment on the Norwegian-Greenland Sea continental margins, Sedimentary Environments Offshore Norway—Palaeozoic to Recent. Norwegian Petroleum Society Special Publications, Elsevier, Berlin, vol 10, pp 451–456
87. Vorren TO, Rydningen TA, Baeten NJ, Laberg JS (2015) Chronology and extent of the Lofoten-Vesterålen sector of the Scandinavian Ice Sheet from 26 to 16 cal. Ka BP. Boreas 44:445–458
88. Wang YY, Zhan XC, Yuan JH, Fan XT (2011) The evaluation of uncertainty in the results for elements rubidium, strontium, yttrium and zirconium in silicate geological samples by polarized energy dispersive X-ray fluorescence spectrometry. Guang Pu Xue Yu Guang Pu Fen Xi 31(6):1707–1711
89. Wilken M, Mienert J (2006) Submarine glacigenic debris flows, deep-sea channels and past ice-stream behaviour of the East Greenland continental margin. Quat Sci Rev 25:784–810
90. Winsborrow MCM, Andreassen K, Corner GD, Laberg JS (2010) Deglaciation of a marine-based ice sheet: Late Weichselian palaeo-ice dynamics and retreat in the southern Barents Sea reconstructed from onshore and offshore glacial geomorphology. Quat Sci Rev 29:424–442
91. Wohlfarth B, Björck S, Possnert G (1995) The Swedish time scale—a potential calibration tool for the radio-carbon time scale during the Late Weichselian. Radio-carbon 37(2):347–60
92. Zecchin M, Rebesco M, Lucchi RG, Caffau M, Lantzsch H, Hanebuth TJJ (2016) Buried iceberg-keel scouring features in the southern Spitsbergenbanken, NW Barents Sea. Mar Geol 382:68–79
93. Zecchin M, Rebesco M (2018) Glacigenic and glacimarine sedimentation from shelf to trough settings in the NW Barents Sea. Mar Geol 402:184–193